Gold nanoparticles as absolute nano-thermometers. Supporting Information

Aquiles Carattino, Martín Caldarola, and Michel Orrit*

Huygens-Kamerlingh Onnes Lab, 2300RA Leiden, The Netherlands

E-mail: orrit@physics.leidenuniv.nl

Anti-Stokes emission from gold nanorods

We model the photoluminescence generation in gold nanorods with successive steps taking place between absorption of light and re-emission of luminescence.[1] Figure S1 shows the energy-momentum representation of the photoluminescence processes in gold nanorods. After excitation with monochromatic light of energy $\hbar\omega_L$, a collective oscillation of electrons is generated, i.e. a surface plasmon. Once the plasmon coherence is lost (dephasing time $\sim$fs), the state can be described as an electron-hole pair. Then, different scenarios are possible: recombination without energy exchange, (i.e. elastic recombination leading to Rayleigh scattering) or recombination with energy exchange. In the latter case, three scenarios are possible: electron and hole may recombine radiatively after one or more interactions with the thermal baths of lattice phonons and charge carrier thermal excitations: i) if the energy difference between electron and hole states is lower than the initial one after excitation we obtain Stokes emission upon a radiative recombination; ii) if electron and hole transiently increase their energy difference at the bath's expense before recombining radiatively, we ob-

serve anti-Stokes emission; iii) if electron and hole recombine non radiatively, their energy difference is transferred to the baths and no photon is emitted. The latter process is the most probable one, explaining the low yield of luminescence in gold nanoparticles ($\sim 10^{-6}$).

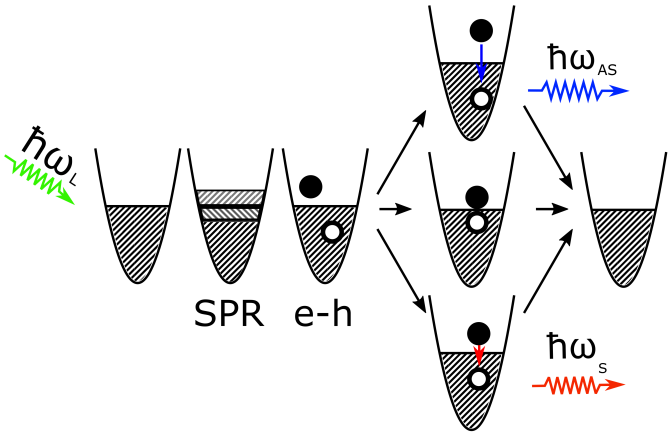

Figure S1: **Schematic representation of Stokes and Anti-Stokes luminescence process from a single gold nanorod.** Upon the excitation with resonant energy $\hbar\omega_{\mathrm{L}}$ a surface plasmon is created, which creates an electron-hole pair state (e-h). This pair can recombine non-radiatively (the most likely event) or radiatively after interacting with the baths, leading emission of a high-energy (anti-Stokes) or low-energy (Stokes) photon.

Determination of the surface plasmon resonance energy

As we mentioned in the main text, the phenomenological model we use to extract the temperature from the anti-Stokes spectrum depends on the prior determination of shape and position of the surface plasmon resonance (SPR). In this paper, we measure the photoluminescence emission spectrum when a single nanorod is excited with a 532 nm CW laser to obtain the SPR. Figure 1 in the main text shows an example of such spectra for an individual nanorod. An asymmetric shape is measured, due to some plasmonic-unrelated contribution from gold[2] added to the plasmonic emission. This complicates the determination of the SPR from the measured spectra, since a simple Lorentzian shape does not fit this data. We present here the way we analyzed the data to circumvent this problem. We first determine this background contribution phenomenologically in independent experiments and then we take it into account for the SPR determination.

We modeled this emission spectra taken with the 532 nm laser with the following phenomenological form

$$I_{\mathrm{PL}}(E) = A_1 B(E;\Delta) + A_2 \mathrm{I}_{\mathrm{SPR}}(E)\,, \tag{1}$$

where E represents the photon energy, B is the broadband contribution from bulk gold, phenomenologically modeled as $B(E;\Delta) = \exp(E/\Delta)$, $\mathrm{I}_{\mathrm{SPR}}(E)$ is the surface plasmon resonance spectrum and A_1, A_2 are constants. We take the $\mathrm{I}_{\mathrm{SPR}}(E)$ to be Lorentzian,[3] i.e.

$$\mathrm{I}_{\mathrm{SPR}}(E) = \frac{(\Gamma/2)^2}{(E - E_{\mathrm{SPR}})^2 + (\Gamma/2)^2}\,. \tag{2}$$

Figure S2(a) presents some individual gold nanorods spectra with size similar to the ones presented in the main text, i.e. a SPR around 630 nm. We use this set of spectra to empirically obtain the shape of the background. Figure S2(b) shows an example of the fitted function and the extracted function $B(E;\Delta)$. We performed this fit on five different nanorods and we averaged the values for Δ, obtaining (0.120 ± 0.02) eV. With the background

defined by this parameter we can extract the $\mathrm{I_{SPR}}(E)$ from the photoluminescence spectra of every individual gold nanorod. For example, the spectra shown in Figure S2 (b) yielded $E_{\mathrm{SPR}} = (1.97 \pm 0.35)$ eV, with a width $\Gamma = (129 \pm 1)$ meV.

For the whole analysis done in the rest of our paper we used this procedure to obtain the surface plasmon resonance profile from the photoluminescence spectrum excited at 532 nm.

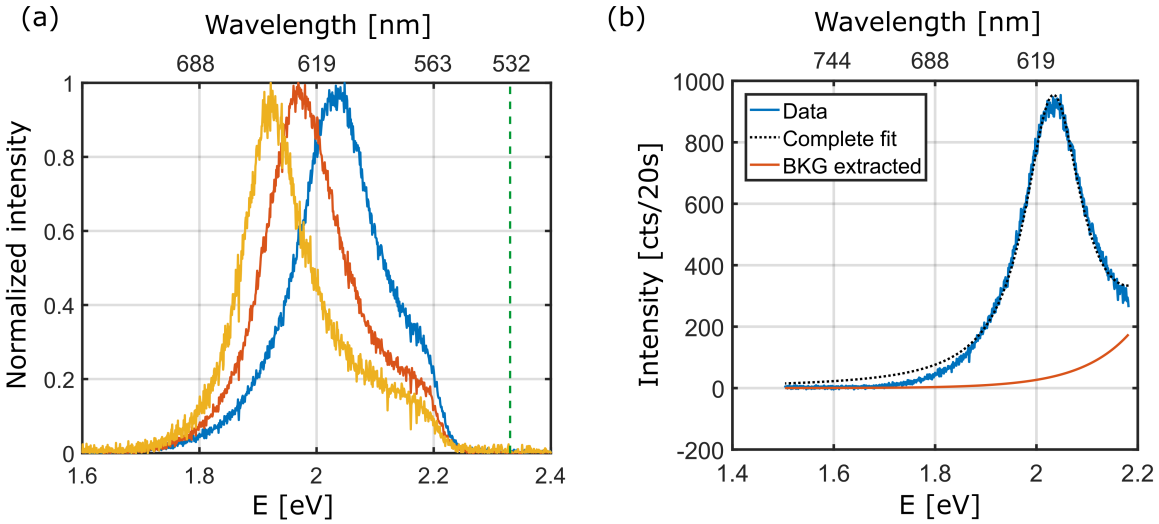

Figure S2: **Photoluminescence spectra of individual gold nanorods.** (a) Normalized emission spectra of three different individual nanorods, all of which present an asymmetric shape due to the bulk emission contribution. The vertical dashed line shows the excitation laser energy and the abrupt cut close to 2.2 eV is due to the notch filter used to prevent laser detection. (b) Example of the fit to extract the function $B(E;\Delta)$. The blue solid line is the spectrum of an individual nanorod and the black dotted line is the fitted function from equation (1). We obtained $E_{\mathrm{SPR}} = (1.97 \pm 0.35)$ eV, with a width $\Gamma = (129 \pm 1)$ meV. The red solid line shows the obtained background function $B(E;\Delta)$, with $\Delta = 0.12$ eV. The integration time of these spectra was 20 s.

The analysis presented above completes the first step in our protocol (presented in the main text).

Experimental setup

The experimental setup consisted of a home-made confocal microscope, schematically shown in Figure S3, similar to the one presented before.[1] The microscope allows the detection of individual nanorods in the sample and the measurement of their photoluminescence spectra. We use continuous wave lasers at 532 nm or 633 nm to excite the transverse and longitudinal plasmon resonances, respectively. The 532 nm source is a DPSS laser (CNI) and the 633 nm one is a HeNe (Thorlabs). Both lasers are reflected at a 50/50 beam splitter and the emitted light from the sample is transmitted. Exchangeable notch filters for both lasers are used accordingly to avoid the detection of the excitation source. This allows the simultaneous detection of both the anti-Stokes and Stokes emission of the particles. The intensity of the 633 nm laser was controlled with an acousto-optical modulator (AA opto-electronics).

We employ an objective lens to focus the excitation beam into a diffraction-limited spot and we collect the emitted photoluminescence using the same objective in an epi-configuration. The 532 nm laser is focused down by our 60× NA1.4 objective to a waist of 228 nm, with a power of 200 μW reaching the sample, leading to an intensity of 1.23 $\mathrm{mW\mu m^{-2}}$. For the HeNe laser, the maximum power used was 100 μWwhich corresponds to 0.43 $\mathrm{mW\mu m^{-2}}$. This is equivalent to 1.37×10^{15} photons $\mathrm{s^{-1}}$ $\mathrm{\mu m^{-2}}$, which leads to a fluence of $\approx 8.2 \times 10^{16}$ photons $\mathrm{\mu m^{-2}}$ in 1 min integration time used for the spectra acquisition. A confocal pinhole of 50 μm is placed between a pair of lenses with 10 cm focal length to reduce the unwanted background from the solvent above the nanorods. Then we could select between an APD or the spectrometer to perform a raster-scan image or an emission spectrum, respectively.

Additionally, the temperature of the sample can be controlled with a special holder that allows water flow, a heater and a thermocouple to measure the temperature of the sample. For the experiments done with this holder we employed an air-spaced 60× objective with NA 0.9 (Olympus) to reduce perturbation of the sample temperature by heat conduction to the objective.

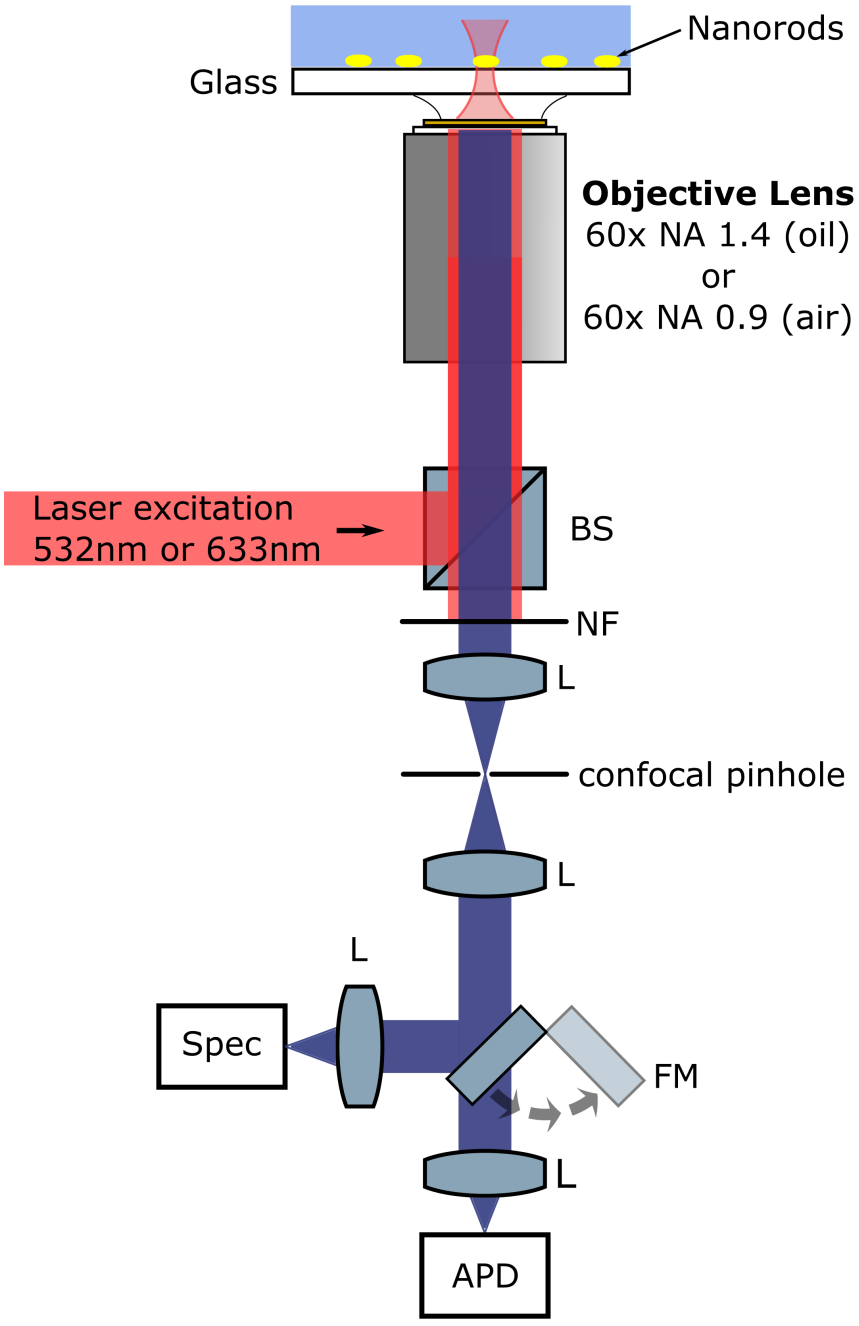

Figure S3: **Scheme of the experimental setup.** The sample consists of individual gold nanorods immobilized on glass. BS: beam splitter. NF: notch filter to remove excitation light and detect Stokes and anti-Stokes photoluminescence. L: lens. FM: flip mirror. SPEC: spectrometer. APD: avalanche photodiode.

Gold nanorods sample characterization

We synthesized gold nanorods using the seed-mediated growth method[4] and characterized their size by performing TEM imaging on a drop-cast sample on a silicon substrate. Figure S4 (a) shows the TEM image and the inset shows a zoom of a cluster of nanorods. In the latter image, the cylindrical shape with spherical caps of the nanorods can be seen. The inset on the right shows the histograms for the length and width obtained from the images. The mean width is (25 ± 5) nm while the mean length is (50 ± 6) nm, leading to a mean aspect ratio of (2.0 ± 0.4).

Naturally, there is some size dispersion due to the fabrication procedure, that leads to a broad bulk extinction spectra, shown in Figure S4 (b). The transverse plasmon resonance is located at 525 nm while the more intense longitudinal plasmon resonance is at 630 nm. We also show the wavelengths of the lasers used for our study as vertical dashed lines.

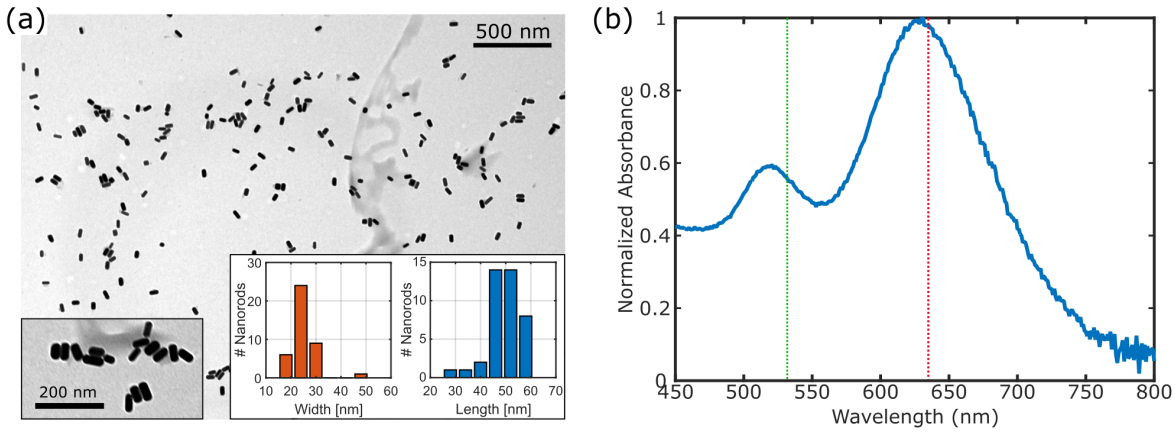

Figure S4: **Gold nanorod characterization.** (a) TEM image of a dried drop of the gold nanorods used in this study. The inset shows higher magnification and the histograms for the width and length. (b) Bulk absorbance spectra of the gold nanorod sample showing the longitudinal surface plasmon resonance around 630 nm. The dashed vertical lines show the two laser wavelengths used in this work.

Luminescence power dependence

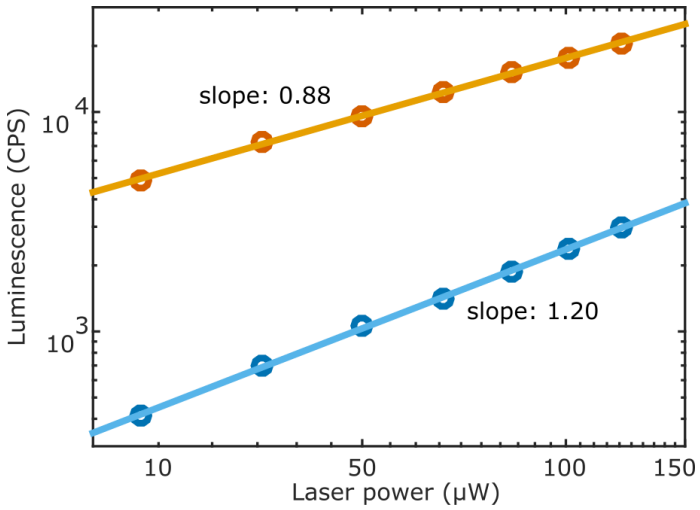

Figure S5: **Stokes and anti-Stokes integrated emission as a function of excitation power.** The linear fits in logarithmic scale have a slope of 0.88 and 1.20 respectively, confirming the 1-photon nature of both kinds of emission.

Figure S5 shows the spectrally-integrated intensity of the Stokes (red) and anti-Stokes (blue) emission for several excitation powers. In both cases the linear fit in logarithmic scale has a slope close to 1, being 0.88 for the Stokes and 1.20 for the anti-Stokes. In order to achieve photon emission at higher energy than the excitation, i.e. an anti-Stokes band, the interaction with the thermal baths has to provide the extra energy required. Since most excitations decay non-radiatively, the energy available in the thermal bath also depends on the previous excitations. Thus, the energy content of the bath also depends on the excitation power, leading to a slope > 1 in Figure S5. In other words, the higher the power, the higher the temperature of the particle and the higher the anti-Stokes signal is. This behavior is independent of the plasmon resonance position. It is important to note that the excitation intensity cannot be increased much beyond what is shown because nanorods would start reshaping towards more spherical shapes at higher laser powers.

Determination of the error in the temperature extraction

In this section we present how we obtain the uncertainty in the temperature determination while using our protocol using an independent set of measurements.

First we get the surface plasmon resonance profile by using the analysis presented before. This gives us the two parameters that characterize the curve, E_{SPR} and Γ with their respective uncertainties. Then we fit the anti-Stokes part of the spectra obtained with nearly resonant excitation of 633 nm, obtaining the curves shown in Figure S6 (a) and the temperature values shown in Figure S6(b). The inset in the Figure S6 (a) shows the SPR spectra obtained in the first step of the procedure.

Secondly, we used the obtained temperature values for each laser power to construct the plot in Figure S6 (b), where the error bars correspond to the square root of the variance of the temperature, estimated by the fitting algorithm. Note that the higher the power, the smaller the error, due to the higher photon counts in the spectra. We emphasize that a single spectrum leads to a temperature value with a relative error of 2 % for powers larger than 70 μW. The highest error is of $\sim 4\%$ for the lowest power used.

We also repeated the temperature extraction using a slightly shifted plasmon resonance energy and we obtained temperatures that differ by around 1 K, which is within the confidence interval presented.

Finally, we performed a linear fit to these temperature values and extrapolated to zero laser power, to obtain the value for the room temperature T_R. We obtained $T_R = (297 \pm 13)\,\mathrm{K}$, consistent with independent measurements of the room temperature.

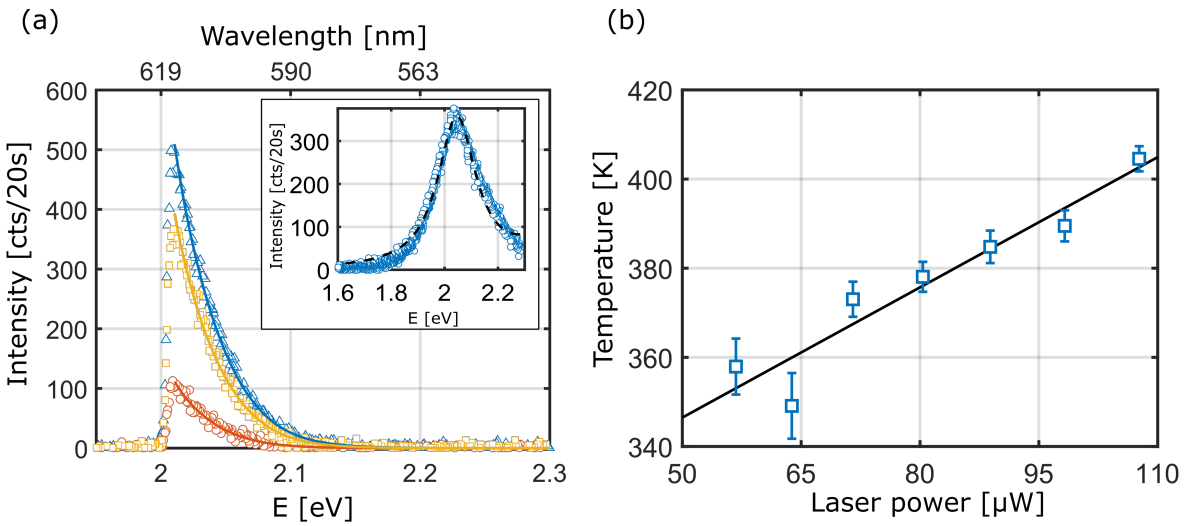

Figure S6: **Temperature extraction from the anti-Stokes emission.** (a) Anti-Stokes spectra for three different 633 nm-excitation powers: 107 μW in blue triangles, 88 μW in yellow squares and 63 μW in red circles. The solid lines correspond to the fit using our model from equation (2) in the main text, with T as a free parameter. The inset shows the photoluminescence spectra of the same nanorod excited with 532 nm (blue circles) and the fit using the equation (1) with a fixed value for Δ (dashed black line), from which we obtained $E_{\mathrm{SPR}} = 2.04$ eV and $\Gamma = 0.175$ eV. The abrupt cut at $E < 2$ eV is due to the notch filter used to prevent laser detection. (b) Temperature extracted from the spectra in (a) for different laser excitation powers. The solid black line corresponds to a linear fit that gives a room temperature value $T_R = (297 \pm 13)\,\mathrm{K}$.

Gold Nanorod temperature numerical calculations

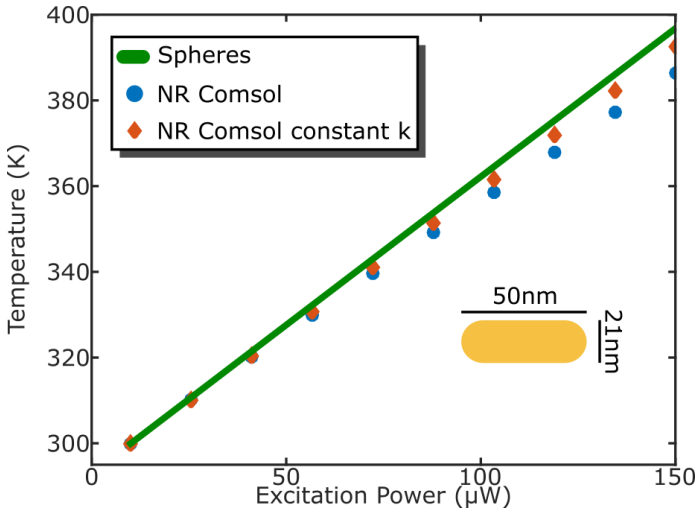

Figure S7: **Gold nanorod temperature calculation for different excitation powers.** Calculated temperature for a nanosphere (full line) and for a 21 nm × 50 nm nanorod (dots) under different excitation intensities. The dots are numerically calculated values using COMSOL Multiphysics commercial software. The blue dots were obtained with the temperature-dependent heat conductivity of water and the red diamonds with a constant value of $0.61\,\mathrm{W(m\cdot K)^{-1}}$.

Throughout the main text the temperature measured with the anti-Stokes emission is compared to the calculated temperature using the heat diffusion equation. For spheres in an homogeneous water environment and assuming an infinite thermal conductivity for the metal, the temperature increase is given by

$$\Delta \mathrm{T}(P) = \frac{P}{4\pi k_{\mathrm{water}} R} \tag{3}$$

where P is the dissipated power, k_{water} is the heat conductivity of water and R is the radius of the particle.[5] The dissipated power can be easily derived from the cross section of the particle at a given wavelength and the intensity of the focused laser beam. For nanorods we assumed an equivalent sphere with radius such that the total rod area is preserved.

Figure S7 shows the difference between the results from the sphere (full line) and a finite element method calculation (dots) for a nanorod of length 50 nm and diameter 21 nm. The

cross section and dissipated power were kept the same. The blue dots are the results given by using the tabulated temperature-dependent heat conductivity of water. The red diamonds are the results when the thermal conductivity is fixed to $0.61\,\mathrm{W}(\mathrm{m}\cdot\mathrm{K})^{-1}$. The difference is accentuated at higher temperatures.

References

(1) Carattino, A.; Keizer, V. I.; Schaaf, M. J.; Orrit, M. Background suppression in imaging gold nanorods through detection of anti-stokes emission. *Biophysical journal* **2016**, *111*, 2492–2499.

(2) Mooradian, A. Photoluminescence of metals. *Phys. Rev. Lett.* **1969**, *22*, 185–187.

(3) Zijlstra, P.; Orrit, M. Single metal nanoparticles: optical detection, spectroscopy and applications. *Reports Prog. Phys.* **2011**, *74*, 106401.

(4) Nikoobakht, B.; El-Sayed, M. A. Preparation and growth mechanism of gold nanorods (NRs) using seed-mediated growth method. *Chem. Mater* **2003**, *15*, 1957–1962.

(5) Baffou, G.; Quidant, R. Thermo-plasmonics: using metallic nanostructures as nano-sources of heat. *Laser Photon. Rev.* **2013**, *7*, 171–187.